Radil controls neutrophil adhesion and motility through β2-integrin activation

Lunhua Liu[a], Wulin Aerbajinai[b], Syed M. Ahmed[c], Griffin P. Rodgers[b], Stephane Angers[c], and Carole A. Parent[a]

[a]Laboratory of Cellular and Molecular Biology, Center for Cancer Research, National Cancer Institute, and [b]Molecular and Clinical Hematology Branch, National Heart, Lung, and Blood Institute, National Institutes of Health, Bethesda, MD 20892; [c]Department of Pharmaceutical Sciences, Leslie Dan Faculty of Pharmacy, University of Toronto, Toronto, ON M5S 3M2, Canada

ABSTRACT **Integrin activation is required to facilitate multiple adhesion-dependent functions of neutrophils, such as chemotaxis, which is critical for inflammatory responses to injury and pathogens. However, little is known about the mechanisms that mediate integrin activation in neutrophils. We show that Radil, a novel Rap1 effector, regulates β1- and β2-integrin activation and controls neutrophil chemotaxis. On activation and chemotactic migration of neutrophils, Radil quickly translocates from the cytoplasm to the plasma membrane in a Rap1a-GTP–dependent manner. Cells overexpressing Radil show a substantial increase in cell adhesion, as well as in integrin/focal adhesion kinase (FAK) activation, and exhibit an elongated morphology, with severe tail retraction defects. This phenotype is effectively rescued by treatment with either β2-integrin inhibitory antibodies or FAK inhibitors. Conversely, knockdown of Radil causes severe inhibition of cell adhesion, β2-integrin activation, and chemotaxis. Furthermore, we found that inhibition of Rap activity by RapGAP coexpression inhibits Radil-mediated integrin and FAK activation, decreases cell adhesion, and abrogates the long-tail phenotype of Radil cells. Overall, these studies establish that Radil regulates neutrophil adhesion and motility by linking Rap1 to β2-integrin activation.**

Monitoring Editor
Mark H. Ginsberg
University of California, San Diego

Received: May 25, 2012
Revised: Sep 13, 2012
Accepted: Oct 18, 2012

INTRODUCTION

Neutrophils are an essential component of the innate immune system and are the first line of defense against bacterial infections (Borregaard, 2010; Wright *et al.*, 2010). The directed migration of neutrophils to sites of inflammation and infection, a process referred to as chemotaxis, is regulated by chemoattractants that signal through pertussis toxin–sensitive G_i-coupled as well as $G_{12/13}$-coupled receptors (referred to as G protein–coupled receptors [GPCRs]; Wang, 2009). Binding of chemoattractants to their specific receptors triggers the dissociation of heterotrimeric G proteins into α and βγ subunits. The βγ subunits are the main transducers of chemotactic signals and activate several downstream effectors, including Ras, PI3K, mTORC2, RhoA, adenylyl cyclase, and phospholipase C, which ultimately lead to the localized polymerization of F-actin at the front of the cell and assembly of myosin II in actomyosin filaments at the sides and rear. F-actin and actomyosin filaments together then provide protrusive and contractile forces that drive chemotaxis (Bagorda and Parent, 2008; Liu *et al.*, 2010; Liu and Parent, 2011).

Cell migration requires the dynamic interaction between cells and the substratum to which they adhere and on which they migrate. The adhesion of neutrophils to the extracellular matrix is mostly mediated via transmembrane integrin receptors, which consist of non–covalently bound heterodimers of α and β chains (Carlos and Harlan, 1994; Chavakis *et al.*, 2009). Mammalian genomes contain 18 α subunits and 8 β subunits genes, and 24 different α–β combinations have been identified (Hynes, 2002; Huttenlocher and Horwitz, 2011). In neutrophils, several integrin heterodimers belonging to the β1, β2, and β3 family are expressed on the cell surface (Berton and Lowell, 1999; Lundberg *et al.*, 2006; Mambole *et al.*, 2010). Integrins on the surface of resting neutrophils normally have low affinity and low avidity for their ligands. Active conformations of integrin receptors on neutrophils can be induced by the binding of

This article was published online ahead of print in MBoC in Press (http://www.molbiolcell.org/cgi/doi/10.1091/mbc.E12-05-0408) on October 24, 2012.

Address correspondence to: Carole A. Parent (parentc@mail.nih.gov).

Abbreviations used: FAK, focal adhesion kinase; fMLP, formyl-Met-Leu-Phe; GPCR, G protein coupled receptor; MLC, myosin regulatory light chain; Radil, RA [Ras associated] and Dil [diluted] domains; RapGAP, Rap GTPase-activating protein; RapGDI, Rap GDP-dissociation inhibitor; RapGEF, Rap guanine exchange factor; RIAM, Rap1-GTP–interacting adaptor molecule.

chemoattractants to GPCRs via inside-out signaling of integrin receptors or by direct ligand binding on integrin receptors via outside-in signaling (Abram and Lowell, 2009).

The Ras-related GTP-binding protein Rap acts as a key mediator of inside-out signaling to the β1, β2, and β3 family integrins. Rap can either assist the transition of integrins into their active forms after agonist addition or maintain integrin activation by preventing active integrins from reverting to their dormant conformations (Kinbara *et al.*, 2003; Bos, 2005). In mammals, five distinct Rap members have been identified: Rap1a, Rap1b, Rap2a, Rap2b, and Rap2c. Their activities are regulated by specific guanine exchange factors (RapGEFs), GTPases activating proteins (RapGAPs), and GDP-dissociation inhibitors (RapGDIs; Raaijmakers and Bos, 2009; Gloerich and Bos, 2011). A number of reports have shown that expression of constitutively active Rap1 promotes integrin activation in T-cells and myeloid cells, whereas inhibition of the activation of endogenous Rap GTP-binding proteins prevents receptor-induced integrin activation (Caron *et al.*, 2000; Katagiri *et al.*, 2000, 2002; Reedquist *et al.*, 2000; Arai *et al.*, 2001; Suga *et al.*, 2001; Abraham, 2002; Sebzda *et al.*, 2002; Shimonaka *et al.*, 2003; Tohyama *et al.*, 2003; Lafuente *et al.*, 2004, 2007). Moreover, in *Dictyostelium discoideum* and *Drosophila melanogaster*, orthologues of the mammalian Rap1 regulate cell morphology, actin polymerization, and cell migration (Rebstein *et al.*, 1993, 1997; Asha *et al.*, 1999; Han *et al.*, 2006; Jeon *et al.*, 2007a,b; Parkinson *et al.*, 2009). Several Rap1 effectors, including regulator for cell adhesion and polarization enriched in lymphoid tissues (RAPL), Rap1–GTP-interacting adapter molecule (RIAM), and a protein containing Arf GAP, Rho GAP, ankyrin repeat, RA, and five PH domains (ARAP3), have been identified and shown to link Rap1 to integrin activation or avidity in various cell types (Katagiri *et al.*, 2003; Lafuente *et al.*, 2004; Gambardella *et al.*, 2011).

A novel Rap downstream effector named Radil (for RA [Ras associated] and DIL [diluted] domains) has been identified (Smolen *et al.*, 2007). Radil is a broadly expressed adapter protein that contains a RA-like domain, a PDZ (postsynaptic density 95, PSD-85; discs large, Dlg; zonula occludens-1, ZO-1) domain and a DIL domain. Like RAPL and RIAM, Radil interacts preferentially with active GTP-bound Rap1, and overexpression of Radil enhances integrin-mediated adhesion. In addition, Radil knockdown inhibits cell–substrate adhesion in HT1080, AD293, and NMuMG cells and results in migration defects in SW1353 and zebrafish neural crest cells (Smolen *et al.*, 2007; Ahmed *et al.*, 2010). Of importance, Radil was found to form a specific complex with Gβγ and Rap1a-GTP, which is important in the regulation of GPCR signaling to cell–matrix adhesion (Ahmed *et al.*, 2010).

In this study, we set out to determine the roles of Rap and Radil during neutrophil adhesion and chemotaxis. We found that Radil regulates neutrophil adhesion by specifically enhancing β2-integrin activation, as well as focal adhesion kinase (FAK) and paxillin phosphorylation. These effects are dependent on Rap activation, as inhibition of Rap by RapGAP rescues the chemotaxis defect of Radil-overexpressing cells and blocks Radil-enhanced integrin activation.

RESULTS

Radil translocates to the plasma membrane during chemotaxis

Radil is a 1075–amino acid protein that directly interacts with active Rap1 (Smolen *et al.*, 2007; Ahmed *et al.*, 2010). By carrying out immunoprecipitation experiments with an antibody directed against Radil (Ahmed *et al.*, 2010), we first established that Radil is expressed in neutrophils and PLB-985 cells—a pluripotent myeloid leukemia cell line that can be terminally differentiated into neutrophil-like cells (Tucker *et al.*, 1987; Supplemental Figure S1A). To determine the cellular distribution of Radil in neutrophils, we generated PLB-985 cells stably expressing Radil-venus (Supplemental Figure S1B). We found that in unstimulated differentiated cells Radil is primarily distributed in the cytoplasm. However, upon uniform stimulation with 1 μM formyl-Met-Leu-Phe (fMLP), Radil transiently translocates to the plasma membrane, peaking ~1 min after agonist addition (Figure 1A and Supplemental Movie S1). This transient translocation was also observed in membranes collected from lysed cells. We found that upon fMLP addition, a significant fraction of Radil becomes associated with membrane fractions, with kinetics that mimic those observed by fluorescence microscopy (Figure 1B). Of interest, when cells were subjected to a gradient of fMLP we found that Radil remains persistently and uniformly distributed on the plasma membrane (Figure 1, C and D, and Supplemental Movie S2). To study the cellular distribution of upstream regulators of Radil, we also expressed venus-tagged wild-type (WT) Rap1a and constitutively active Rap1a (Rap1aQ63E), as well as cerulean-tagged Rap1GAP, in PLB-985 cells (Supplemental Figure S1B). We found that Rap1aWT and Rap1aQ63E remain uniformly distributed in the cytoplasm in both resting and migrating cells (Figure 1C). In the resting state, Rap1GAP also remains cytoplasmic. However, during chemotaxis, Rap1GAP becomes enriched at the front of migrating cells (Figure 1C).

Rap1a-GTP and Radil regulate back-retraction in chemotaxing neutrophils

To determine the role of Radil during neutrophil chemotaxis, we assessed the chemotactic ability of Radil-overexpressing cells. We also studied Rap1aQ63E- and Rap1GAP-overexpressing cells to assess the effect of the gain or loss of Rap1 function on neutrophil chemotaxis. The Rap1aWT cells, which behave similarly to the parental PLB-985 cells and venus-expressing cells (Supplemental Figure S2, A and B), were used as control. To assess chemotaxis, we used the EZ-Taxiscan system, which allows the visualization of cell migration in shallow, linear gradients of fMLP over long distances (Nitta *et al.*, 2007). We found that Radil and Rap1aQ63E cells display a dramatically elongated cell shape during chemotaxis on both BSA- and fibronectin-coated surfaces (Figure 2A and Supplemental Movie S3, as well as unpublished data). Morphometric measurements show that, in their resting state, both Radil and Rap1aQ63E cells are round, with a circularity of 0.81 ± 0.08, which is comparable to values obtained for Rap1aWT and Rap1GAP cells (Figure 2B, zero time point). Two minutes after the initiation of chemotaxis, the circularity of all four cell lines gradually decreased as the cells adhered and extended pseudopods. After 10 min, Rap1aWT and Rap1GAP cells were fully polarized, and their circularity was further decreased to 0.52 ± 0.05 and 0.51 ± 0.07, respectively. Both cell lines maintained a similar degree of circularity until 20 min (Figure 2B). In sharp contrast, a significant decrease in cellular circularity was measured in both Radil and Rap1aQ63E cells, in which the circularity after 20 min decreased to 0.15 ± 0.02 and 0.19 ± 0.04, respectively (Figure 2B). For these two cell lines, these elongated shapes could be a consequence of defects in back detachment or tail retraction. Indeed, quantification of back and tail length showed a greater than threefold increase in both Radil and Rap1aQ63E cells compared with Rap1aWT control cells (Figure 2C).

Because Radil and Rap1aQ63E cells exhibit abnormal back and tail morphology and detachment, we next assessed whether their chemotactic ability is also impaired. Quantification by cell tracking revealed that all four cell lines exhibit similar velocity and directionality during the first 5 min of chemotaxis (Figure 2, D and E).

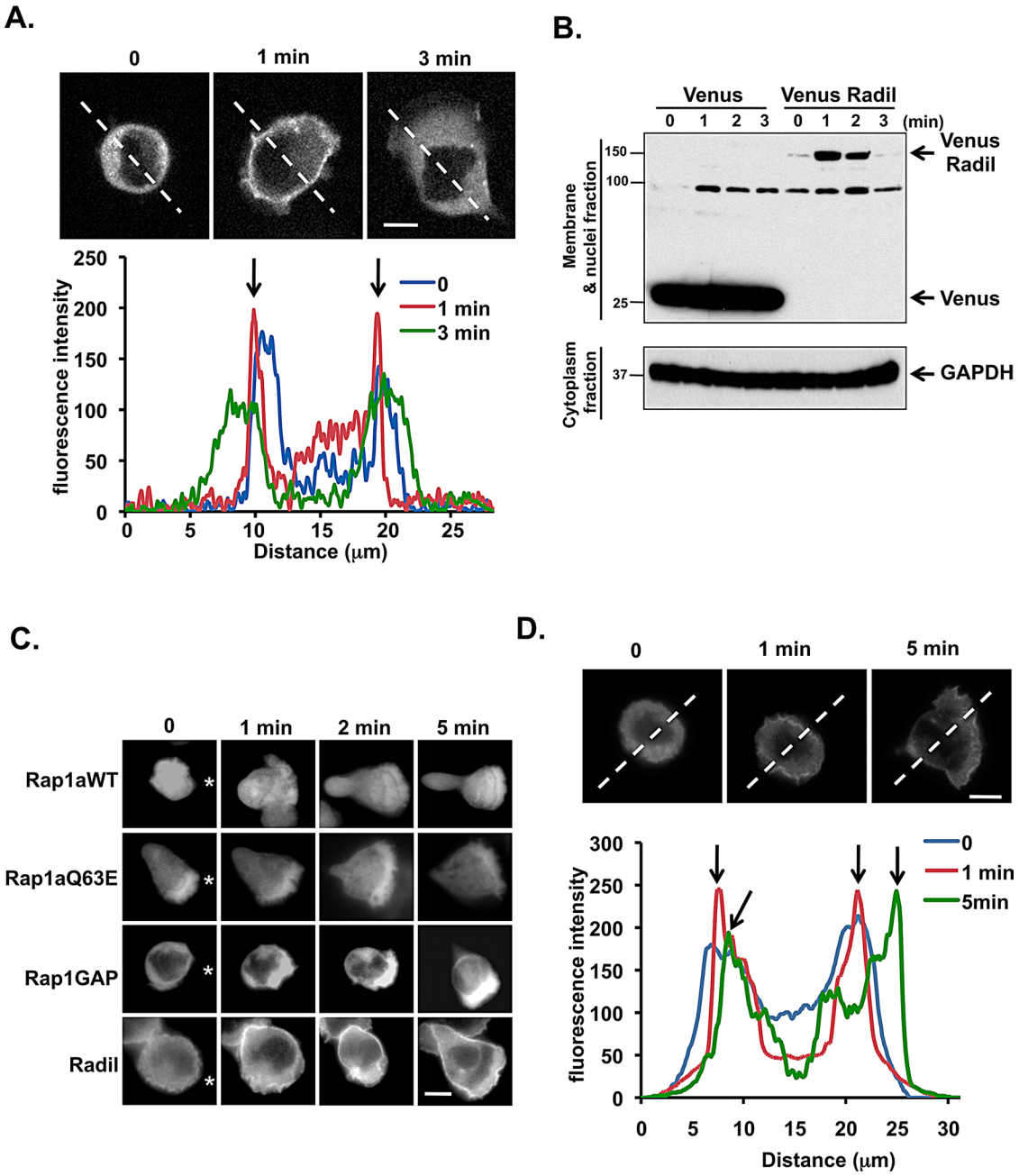

FIGURE 1: Radil translocates to the plasma membrane in response to fMLP addition. (A) Subcellular localization of Radil after uniform fMLP addition. Still fluorescence images from time-lapse recordings of Radil cells before and after the addition of 1 μM fMLP. Venus fluorescence intensity was determined by line-scan analysis (white line) at the indicated time points. The arrows represent the fluorescence intensity peaks on the plasma membrane in the 1-min frame. Bar, 10 μm. Also see Supplemental Movie S1. (B) Translocation kinetics of Radil to the plasma membrane after uniform fMLP stimulation. Differentiated venus and Radil cells were uniformly stimulated with 1 μM fMLP. At specific time points, membrane and cytosol fractions were isolated and subjected to Western blot analysis using an antibody against GFP. A representative blot of three independent experiments is shown. (C) Cellular localization of Rap1aWT, Rap1aQ63E, Rap1GAP, and Radil in chemotaxing neutrophils. Still fluorescence images from time-lapse recordings of chemotaxing cells are presented. The star indicates the position of the micropipette containing 1 μM fMLP. Bar, 10 μm. (D) Translocation kinetics of Radil to the plasma membrane in chemotaxing neutrophils. Cells were treated as in C. The venus fluorescence intensity was determined by line-scan analysis (white line) at the indicated time points. Bar, 10 μm. The arrows represent the fluorescence intensity peaks on the plasma membrane in the 1- and 5-min frames. Also see Supplemental Movie S2.

However, compared with Rap1aWT cells, the speed and directionality of Radil and Rap1aQ63E cells are significantly decreased during the following 15 min of directed migration (Figure 2, D and E). Of interest, we also observed a slight decrease in both velocity and directionality for Rap1GAP cells during the later phase of migration. Taken together, these findings show that Rap1 activity and Radil are important to maintain normal back retraction and morphology during neutrophil chemotaxis.

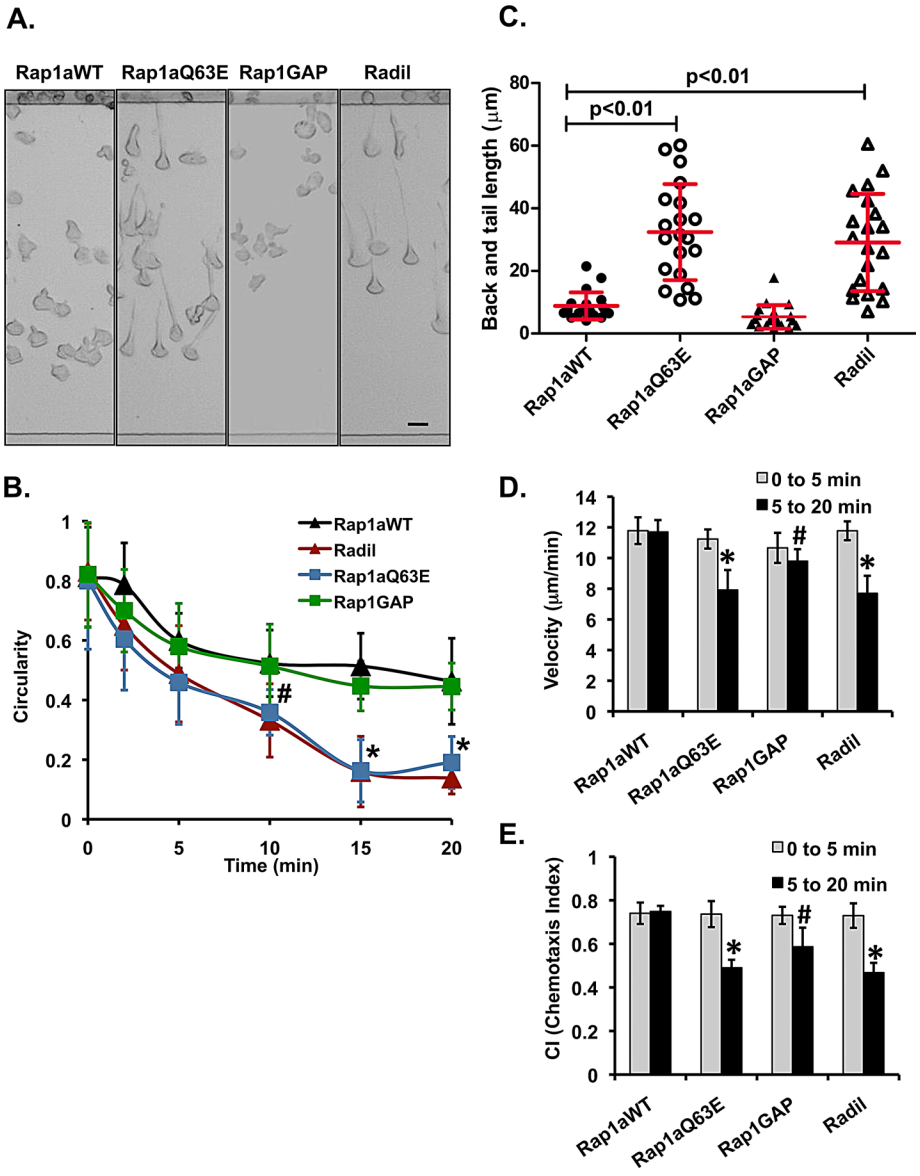

FIGURE 2: Radil and Rap1aQ63E cells have long tails and exhibit chemotaxis defects. (A) Radil cells have long tails during chemotaxis. Still images from EZ-Taxiscan recordings of Rap1aWT, Rap1aQ63E, Rap1GAP, and Radil cells. Also see Supplemental Movie S3. Bar, 10 μm. (B) Chemotaxing Radil and Rap1aQ63E cells are elongated. Cell circularity was quantified from the EZ-Taxiscan recordings and plotted as a function of time. Mean ± SD from five independent experiments. *$p < 0.01$; #$p < 0.05$. (C) Chemotaxing Radil and Rap1aQ63E cells have long tails. The length of the back and tail of the chemotaxing cells was quantified from the EZ-Taxiscan recordings using ImageJ. Mean ± SD. Each point represents measurements from randomly selected cells of one experiment ($n = 20$). (D) Chemotaxing Radil and Rap1aQ63E cells have decreased migration speed. Migration speed of cells during the first 5 min and from 5 to 20 min was quantified from the EZ-Taxiscan recordings. The graph represents mean ± SD from five independent experiments. *$p < 0.01$; #$p < 0.05$. (E) Chemotaxing Radil and Rap1aQ63E cells have lower chemotaxis index (CI). The CI of cells during the first 5 min and from 5 to 20 min was quantified from EZ-Taxiscan recordings. The graph represents mean ± SD from five independent experiments. *$p < 0.01$; #$p < 0.05$.

Rap1a-GTP and Radil regulate neutrophil adhesion

Neutrophil tail retraction is regulated through the RhoA-mediated, ROCK-dependent phosphorylation of the regulatory light chain of myosin II (MyoII; Niggli, 1999; Xu *et al.*, 2003), which occurs in a cAMP- and mTORC2-dependent manner (Liu *et al.*, 2010). To determine whether the abnormal back morphology of Radil and Rap1aQ63E cells results from a defect in signals leading to MyoII phosphorylation, we measured cAMP production, RhoA activation, and myosin regulatory light chain (MLC) phosphorylation after fMLP addition in these cells. We found that Radil and Rap1aQ63E cells have similar low basal intracellular cAMP levels compared with Rap1aWT and Rap1GAP cells and exhibit a similar increase in intracellular cAMP levels after fMLP addition (Figure 3A). We also found that in all four cell lines, fMLP exposure leads to a drop in RhoA activity after 1 min, followed by an increase in activity at 5 min (Figure 3B and Supplemental Figure S3A). Furthermore, we observed that all cell lines display comparable fMLP-induced MLC phosphorylation levels, as well as normal F-actin assembly (Figure 3C and Supplemental Figure S3, B and C). Taken together, these findings show that all four cell lines normally transduce signals from fMLP to MLC phosphorylation and that the abnormal back morphology of Radil and Rap1aQ63E cells does not result from defects in signals that lead to myosin II phosphorylation. These findings also establish that Rap signaling is not involved in regulating F-actin assembly in response to fMLP stimulation.

The tail-retraction defects of Radil and Rap1aQ63E cells could also result from cell–surface adhesion defects. Indeed, effective chemotaxis not only requires neutrophils to retract their tails, but it also requires a highly regulated control of adhesion forces with the surface. We therefore assessed whether Radil regulates neutrophil adhesion. First, we observed that cells overexpressing Radil or Rap1aQ63E are flatter and more spread compared with Rap1aWT control cells (Figure 3D). This phenotype is dramatically reduced in cells overexpressing Rap1GAP or a dominant-negative mutant of Rap1 (RapS17N) (Figure 3D and unpublished data), suggesting that Radil may regulate neutrophils adhesion. This conclusion was further confirmed using cell adhesion assays, which measure the fraction of cells that attach to fibronectin-coated surfaces after controlled agitation. We found that, compared with Rap1aWT control cells, Radil and Rap1aQ63E cells exhibit enhanced cell adhesion in response to fMLP addition (Figure 3E and Supplemental Figure S3D). In contrast, Rap1GAP and RapS17N cells showed reduced adhesion under similar conditions (Figure 3E and unpublished data). Thus the abnormal back morphology of Radil and Rap1aQ63E cells may be a consequence of their strong cell–surface adhesion.

Rap1a-GTP and Radil regulate β1- and β2-integrin activation

Adhesion of neutrophils is a dynamic process regulated through the interaction of integrin receptors with extracellular matrix

components (Rose *et al*., 2007). The activation of integrin receptors is partially controlled by Rap1 through an inside-out signaling process (Bos *et al*., 2003; Bos, 2005; Banno and Ginsberg, 2008). Having established that the overexpression of Radil or Rap1aQ63E enhances neutrophil adhesion, we investigated whether Radil regulates cell–substrate adhesion through inside-out signaling and integrin activation. To get at this, we took advantage of the conformationally sensitive monoclonal antibodies that selectively recognize activated β1- and β2-integrins (see *Materials and Methods*). We found that after fMLP treatment, a substantial increase in active β1- and β2-integrin occurs in both dPLB-985– and Rap1aWT-overexpressing cells (Supplemental Figure S4A and Figure 4, A and B). Of importance, and consistent with the requirement of activated Rap1a for integrin activation, we found that the overexpression of Radil or Rap1aQ63E dramatically enhances β1- and β2-integrin activation, whereas overexpression of Rap1GAP inhibits β1- and β2-integrin activation (Figure 4, A and B).

Activated integrins recruit FAK, where it is autophosphorylated on Tyr-397 and functions as a phosphorylation-regulated scaffold to recruit Src to focal adhesions. Src, in turn, phosphorylates a wide array of targets, including paxillin, to coordinate downstream signaling (Burridge *et al*., 1992; Guan, 1997; Thomas *et al*., 1999; Guo and Giancotti, 2004; Webb *et al*., 2004; Mitra and Schlaepfer, 2006). To address whether Radil can regulate integrin signaling events, we measured the effect of Radil on FAK and paxillin phosphorylation after fMLP stimulation. We found that expression of Radil or Rap1aQ63E enhances phosphorylation of FAK and paxillin relative to cells expressing Rap1aWT (Figure 4, C and D, and Supplemental Figure S4B). In contrast, and consistent with our findings on β1- and β2-integrin activation (Figure 4, A and B), fMLP addition gave rise to only modest FAK and paxillin phosphorylation in Rap1GAP cells (Figure 4, C and D, and Supplemental Figure S4B). To determine whether increased FAK signaling plays a role in the chemotaxis defect of Radil cells, we performed EZ-Taxiscan chemotaxis assays on cells treated with the FAK inhibitors PF-573228 and FAK inhibitor 14. We envisioned that if the long-tail and aberrant chemotaxis defects of the Radil cells are a consequence of high FAK phosphorylation levels, FAK inhibition should rescue these defect. We found that treatment with either inhibitor effectively rescues the abnormal tail morphology of Radil cells (Figure 4, E and F, and Supplemental Movie S4). Moreover, FAK inhibition enhanced the chemotaxis ability of Radil cells (Supplemental Figure S4C and Supplemental Movie S4). Taken together, these findings suggest that Rap1a-GTP and Radil regulate neutrophil chemotaxis through their effect on integrin activation and FAK phosphorylation.

Radil regulates neutrophil adhesion and chemotaxis by controlling β2-integrin activation

To identify which integrin is responsible for the increased cell adhesion and impaired chemotaxis of Radil cells, we measured the effects of β1- and β2-integrin–blocking antibodies on adhesion and chemotaxis of Radil cells. We found that the addition of anti-β2 antibodies alone or in combination with anti-β1 antibodies significantly decreases the adhesion of Radil cells, whereas anti-β1 antibodies alone have modest effects (Figure 5A), indicating that the enhanced cell adhesion is mediated through β2-integrin activation. Moreover, the addition of anti-β2 antibodies reduced the abnormal back and tail morphology of Radil cells alone or in combination with anti-β1 antibodies, whereas anti-β1 antibodies again had more modest effects (Figure 5, B–D, and Supplemental Movie S5). Consistently, we found that anti-β2 antibodies and the combination of anti-β1 with anti-β2 antibodies increase the migration directionality and velocity of Radil cells, whereas control isotope immunoglobulin G (IgG) and anti-β1 antibodies have no effect (Supplemental Figure S5A). Collectively, these findings demonstrate that Radil regulates neutrophil adhesion and chemotaxis by primarily modulating β2-integrin activation.

To gain insight into how Radil regulates integrins, we next determined the cellular distribution of total and active β2-integrins in fMLP-stimulated neutrophils. We found that active β2-integrins are mostly localized at the rear of polarized primary human blood neutrophils in the form of punctates, away from the F-actin–rich leading edge (Supplemental Figure S5B). Furthermore, a three-dimensional reconstruction of *Z*-stack slices shows minimal active β2-integrin surface labeling (Supplemental Figure S5C). Indeed, in contrast to mesenchymal cells, neutrophils rely on very dynamic and relatively weak cell–substrate adhesion forces when migrating in two dimensions (Friedl *et al*., 1998; Friedl and Wolf, 2010). Similarly, in Rap1aWT cells, active β2-integrins also appear as punctates at the rear and tail of polarized cells (Figure 5, E and F). Of interest, the overexpression of Radil did not change the asymmetrical distribution of active β2-integrins but markedly enhanced the overall activated β2-integrin fluorescent signal, where several punctate are readily observed in these cells compared with the Rap1aWT cells (Figure 5, E and F).

To substantiate the role of Radil in β2-integrin regulation, we knocked down Radil expression in PLB-985 cells using small interfering RNA (siRNA). We observed a significant knockdown of the level of endogenous Radil with three independent siRNAs (Figure 6A). As expected, Radil-knockdown cells showed a dramatic decrease in their ability to adhere to fibronectin-coated surfaces in response to fMLP stimulation and a dramatic decrease in the cellular amount of active β2-integrins compared with either WT or scramble siRNA cells (Figure 6, B and C). The functional consequence of these defects was readily observed by the inability of the knockdown cells to migrate directionally in a gradient of fMLP (Figure 6D and Supplemental Movie S6). Whereas WT and scramble siRNA cells showed robust chemotaxis, few knockdown cells made it out of the chamber, and the ones that did appeared to randomly migrate over very short distances. Taken together, these findings strongly suggest that Radil controls neutrophil chemotaxis by regulating β2-integrin signaling at the rear of polarized neutrophils.

Rap activation is required to mediate the effects of Radil on neutrophil adhesion and chemotaxis

Radil was recently described as a Rap effector (Smolen *et al*., 2007; Ahmed *et al*., 2010), and Rap activation has been implicated in inside-out signaling leading to the activation of integrins and increases in cell–surface adhesion (Bos *et al*., 2003; Bos, 2005). Thus we next sought to determine whether Rap activation is required to mediate the effects of Radil on neutrophil adhesion and chemotaxis. We coexpressed Rap1GAP, a negative regulator of Rap, in our Radil cells and measured fMLP-mediated adhesion and chemotaxis in these cells. As controls, we coexpressed Rap1GAP with Rap1aWT or Rap1aQ63E. As expected, we found that coexpression of Rap1GAP and Rap1aWT inhibits fMLP-mediated adhesion compared with Rap1aWT cells (Figure 7A). However, the inhibition was not complete (compare with Figure 6B for the Radil siRNA cells), and the Rap1GAP/Rap1aWT-coexpressing cells could still migrate directionally in a gradient of fMLP, albeit with less directionality (unpublished data). Again as expected, coexpression of Rap1GAP with the constitutive mutant of Rap1a, Rap1aQ63E, did not alter the adhesion profile compared with Rap1aQ63E cells (Figure 7A). Taken together, these findings establish that the overexpression of Rap1GAP negatively regulates Rap1a activity.

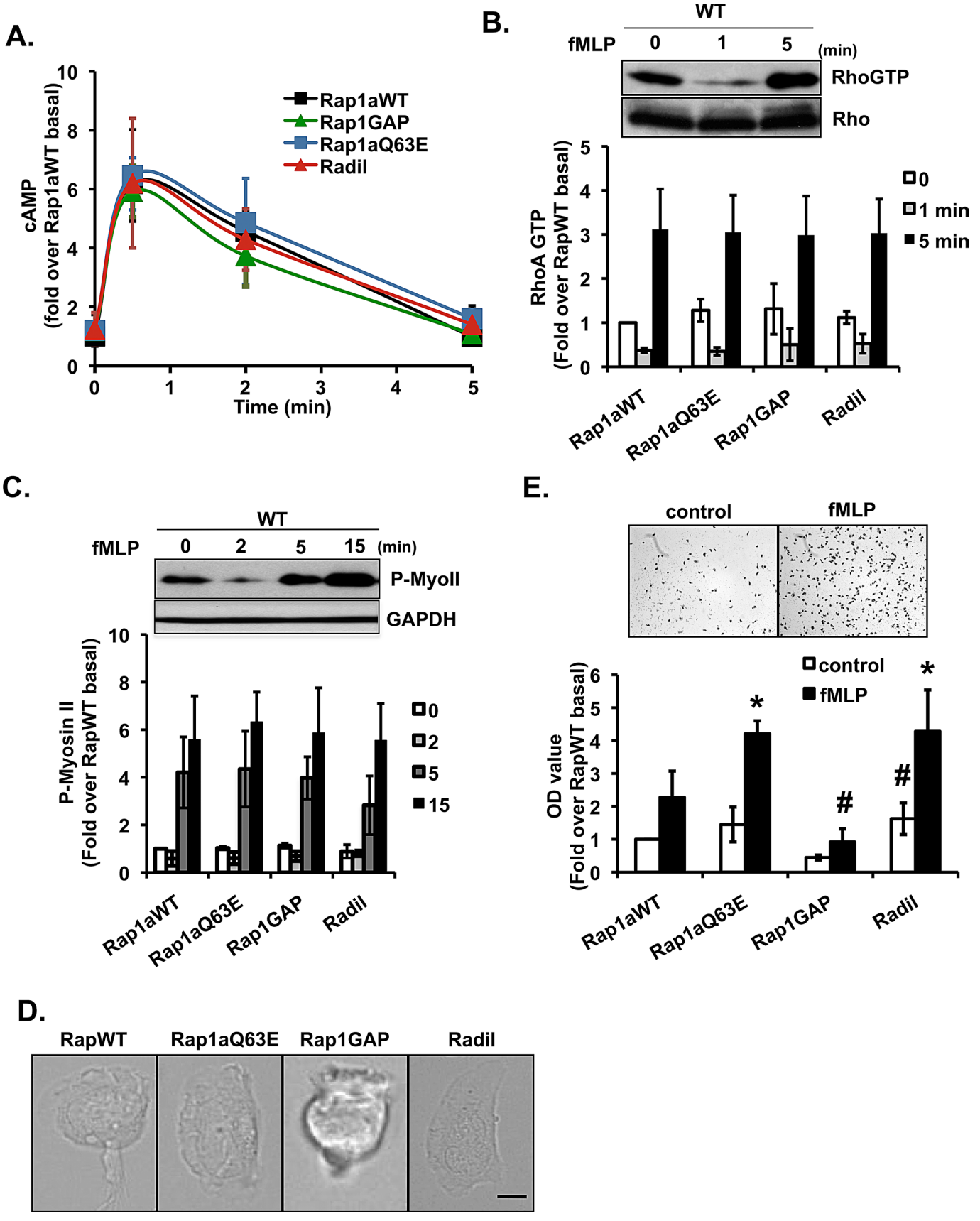

FIGURE 3: Radil and Rap1aQ63E cells exhibit enhanced fMLP-mediated cell–matrix adhesion. (A) Rap1GAP, Radil, and Rap1aQ63E cells have normal AC9 activity. Cells were uniformly stimulated with 1 μM fMLP, and intracellular cAMP levels were measured at the indicated time points. The graph represents mean ± SD from three independent experiments. (B) Rap1GAP, Radil, and Rap1aQ63E cells show normal RhoA activity. Cells were plated on

The Rap1GAP/Radil-coexpressing cells showed a dramatic decrease in adhesion compared with Radil cells (Figure 7A). We also observed that the coexpression of Rap1GAP reduced the high β1/β2-integrin activity and fMLP-mediated FAK and paxillin phosphorylation levels measured in Radil cells without significantly affecting the Rap1aQ63E cells (Supplemental Figure S6, A–C, and Figure 7, B and C). Consistent with these findings, we found that Rap1GAP only abrogated the long-tail phenotype when coexpressed with Radil but not with Rap1aQ63E (Figure 7, D and E, Supplemental Figure S7A, and Supplemental Movie S7). Moreover, Rap1GAP expression restored the migration directionality and velocity to normal levels when coexpressed with Radil cells (Supplemental Figure S7, B and C). Taken together, these data show that Rap activation is required to mediate the effects of Radil, as inactivation of Rap is sufficient to rescue the adhesion and motility defects of Radil-overexpressing cells.

We next assessed the subcellular localization of Radil when it is coexpressed with Rap1GAP. In contrast to what we observed in Radil cells (Figure 1A), when we stimulated the Rap1GAP/Radil cells with fMLP we found that Radil remains uniformly distributed in the cytoplasm (Figure 7F and Supplemental Figure S7, D and E). Yet Rap1GAP is enriched at the front of chemotaxing Rap1GAP/Radil and Rap1GAP/Rap1aQ63E cells (Supplemental Figure S7D), similarly to what we observed in cells expressing Rap1GAP (Figure 1C). Thus, as previously reported in other cell types, the membrane translocation of Radil in neutrophils is dependent on active Rap (Ahmed *et al.*, 2010). Collectively, these findings show that the inhibition of Rap1 by overexpression of Rap1GAP not only inhibits the membrane translocation of Radil, but also leads to the inhibition of Radil-mediated integrin activation, signaling to FAK and paxillin, and the formation of long tails during chemotaxis.

DISCUSSION

We identified Radil as a novel regulator of β2-integrin–mediated adhesion that controls neutrophil tail retraction and chemotaxis. We also established that Radil regulates integrin signaling through FAK activation in neutrophils and that inhibition of FAK, as well as β2-integrin signaling, is sufficient to rescue the tail retraction and chemotaxis defects of neutrophils overexpressing Radil. Previous studies suggested that Radil is an effector of Rap, displaying a preference for active Rap and modulating Rap-dependent biological processes (Ahmed *et al.*, 2010). Consistent with this, our findings strongly suggest that the effects of Radil on neutrophil adhesion and chemotaxis depend on Rap1, as the inhibition of Rap1 rescues the chemotaxis defects of Radil cells.

Although it has been reported that active β2-integrins localize to the leading edge of differentiated HL-60 cells (He *et al.*, 2011), consistent with earlier findings (Pierini *et al.*, 2000), we found that active β2-integrins appear in punctates that do not colocalize with F-actin and are generally enriched in the back of polarized primary human blood neutrophils and differentiated PLB-985 cells. Of importance, polarized PLB-985 cells overexpressing Radil show a significant increase in fluorescent signal of active β2-integrins at their back. Conversely, we measured a significant decrease in the fMLP-mediated adhesion, as well as in the level of active β2-integrin in Radil-knockdown cells, which leads to dramatic migration defects. Thus we propose that Radil specifically regulates cell–substrate attachments at the back of cells. In this context, overexpression of Radil results in excessive localized activation of integrins, as well as the formation of long tails during chemotaxis, and Radil-knockdown cells show the opposite phenotype, with low integrin activation and generalized migration defects.

Much like Radil, the Rap1 effectors RIAM and RAPL have been shown to regulate adhesion and integrin activation (Katagiri *et al.*, 2003; Lafuente *et al.*, 2004). However, in contrast to RIAM and RAPL, which are localized to the leading edge of polarized cells, the addition of fMLP leads to a redistribution of Radil from the cytosol to the entire plasma membrane of neutrophils and HT1080 cells (Ahmed *et al.*, 2010). This difference most probably results from the distinct domain organization of RIAM, RAPL, and Radil. Although all of these effectors contain RA or RBD domains that help them to selectively bind to active Rap1, RIAM also contains a PH domain and a profilin-binding motif that can interact with phosphatidylinositol 3,4,5-triphosphate and profilin, respectively, and recruit RIAM to the leading edge of polarized cells (Lafuente *et al.*, 2004). Alternatively, RAPL may be redistributed to the leading edge by direct interaction with LFA1 (Katagiri *et al.*, 2003). On the other hand, Radil has been shown to form a complex with Gβγ and Rap1a-GTP that regulates GPCR-mediated cell–matrix adhesion (Ahmed *et al.*, 2010). In neutrophils, similar to what we observe with Radil, Gβγ complexes remain uniformly distributed on the plasma membrane after chemoattractant addition (Chen *et al.*, 2008). We envision that chemoattractant addition leads to the release of Gβγ subunits and the activation of Rap1a, which binds to Radil and forms an active Gβγ-Radil-Rap1a-GTP complex that provides spatiotemporal control of the activation process. Indeed, our data suggest that there is a requirement for Gβγ for the activation of Radil, as the overexpression of Radil (or Rap1aQ63E) did not alter basal measurements, including β2-integrin activation.

fibronectin-coated plates for 10 min and uniformly stimulated with 1 μM fMLP, and RhoA-GTP was pulled down and detected using a RhoA antibody. Quantification of three experiments is presented as the amount of RhoA-GTP after fMLP stimulation relative to that of Rap1aWT unstimulated cells (mean ± SD). The amount of RhoA-GTP at each point was standardized by dividing its value with the value of total RhoA of the same time point. Top, time-course measurement of active RhoA in Rap1aWT cells. Also see Supplemental Figure S3A for a representative Western blot. (C) Rap1GAP, Radil, and Rap1aQ63E cells show normal myosin II phosphorylation. Cells were plated on fibronectin-coated plates for 10 min and uniformly stimulated with 1 μM fMLP, and phosphorylated (P)-MLC was assessed at specific time points. Quantification of three experiments is presented as the amount of P-MLC after fMLP stimulation relative to that of unstimulated Rap1aWT cells (mean ± SD). The amount of P-MLC at each point was standardized by dividing its value with the value of GAPDH of the same time point. Top, time-course measurement of P-MyoII in Rap1aWT cells. Also see Supplemental Figure S3B for a representative Western blot. (D) Radil and Rap1aQ63E cells are flatter than Rap1aWT cells. Representative differential interference contrast images of chemotaxing cells. Bar, 10 μm. (E) Radil and Rap1aQ63E cells strongly adhere to fibronectin-coated surfaces. Cell adhesion assays were performed as described in *Materials and Methods*. Quantification of three independent experiments is presented (mean ± SD). Values are presented as fold over Rap1aWT cell basal levels (see Supplemental Figure S3D). Top, a representative image of adhesive Rap1aWT cells before and after fMLP stimulation. $^{*}p < 0.01$; $^{\#}p < 0.05$.

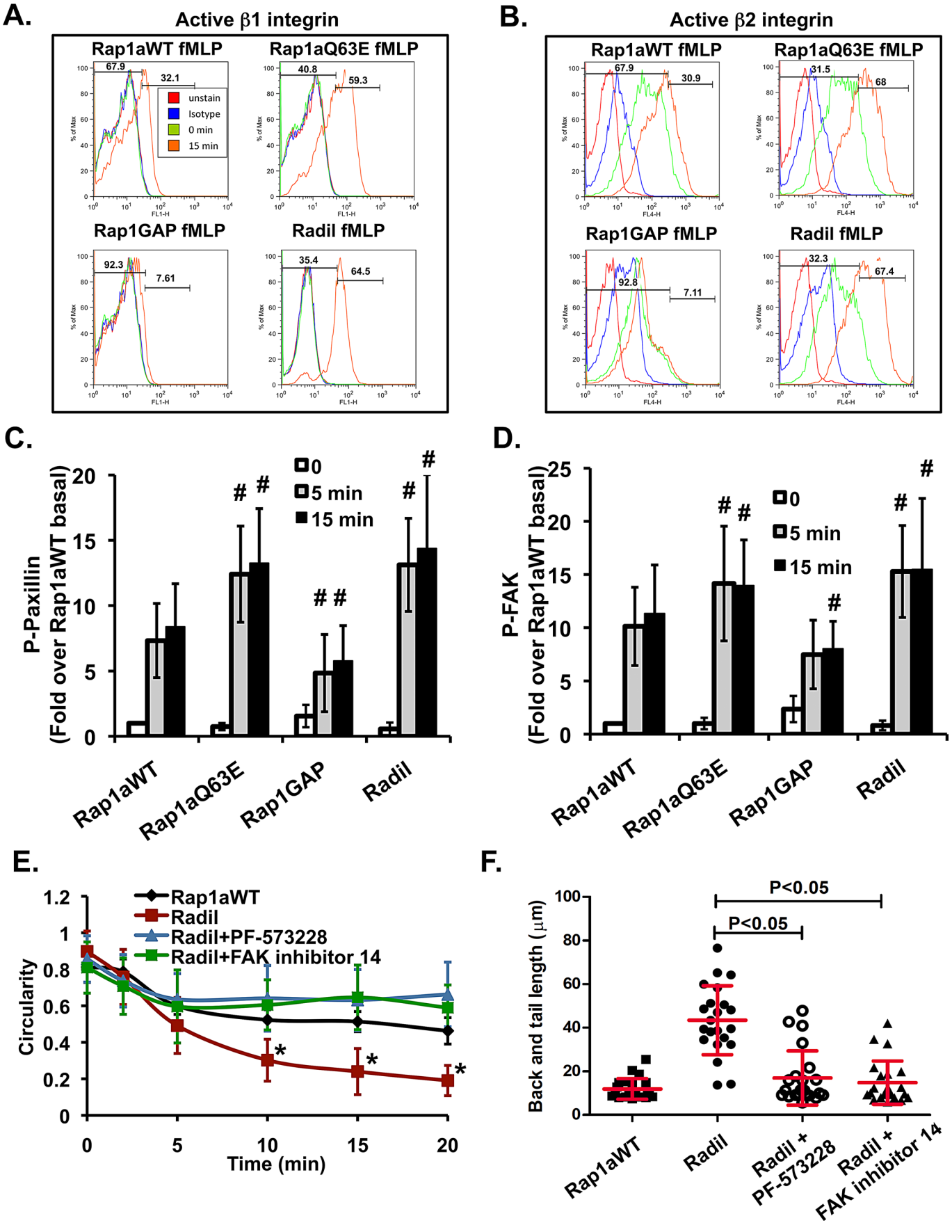
A.
Active β1 integrin
Rap1aWT fMLP
Rap1aQ63E fMLP
Rap1GAP fMLP
Radil fMLP
67.9
32.1
40.8
59.3
92.3
7.61
35.4
64.5
unstain
Isotype
0 min
15 min
% of Max
FL1-H
B.
Active β2 integrin
Rap1aWT fMLP
Rap1aQ63E fMLP
Rap1GAP fMLP
Radil fMLP
67.9
30.9
31.5
68
92.8
7.11
32.3
67.4
FL4-H
C.
P-Paxillin
(Fold over Rap1aWT basal)
0
5 min
15 min
Rap1aWT
Rap1aQ63E
Rap1GAP
Radil
D.
P-FAK
(Fold over Rap1aWT basal)
E.
Circularity
Time (min)
Rap1aWT
Radil
Radil+PF-573228
Radil+FAK inhibitor 14
F.
Back and tail length (μm)
P<0.05
P<0.05
Rap1aWT
Radil
Radil + PF-573228
Radil + FAK inhibitor 14

Rap1a-deficient neutrophils have been generated (He *et al.*, 2011) and, much like what we observed with our Radil-knockdown cells, shown to exhibit decreased adhesion on fibrinogen-coated plates. Of interest, these authors observed that Rap1a-depleted neutrophils retract slowly and show spindle-shaped morphology during chemotaxis. In contrast, our Radil-knockdown cells show a generalized inability to migrate efficiently. He *et al.* (2011) suggested that the elongated-morphology phenotype of the Rap1a-depleted cells results from the inability of these cells to form tight adhesions at their leading edge, which causes back retraction defects. Given that Radil is just one of many Rap1a effectors, the phenotype of Rap1a-deficient cells will undoubtedly be complex. We propose that the specific lost of back adhesions in Radil-deficient neutrophils gives rise to cells that cannot efficiently migrate because of an inability to secure back adhesions.

The chemoattractant-mediated membrane localization of Radil is likely to be critical for its function. We found that the translocation of Radil to the plasma membrane is dependent on the presence of active Rap1, as the overexpression of Rap1GAP abrogates this response. Most important, Rap1GAP expression also inhibits the ability or Radil to increase adhesion and integrin activation. Although in chemotaxing neutrophils we do not detect Rap1 redistribution to the plasma membrane, we foresee that only active Rap1, which represents a small portion of Rap1, redistributes to the plasma membrane of chemoattractant-stimulated neutrophils. Similar results have been reported in *Dictyostelium*, where, in response to chemoattractant stimulation, the active Rap1 reporter RalGDS–yellow fluorescent protein transiently redistributes to the plasma membrane (Jeon *et al.*, 2007b)—a response that is barely observed using green fluorescent protein (GFP)–Rap1 without removing the soluble cytoplasmic GFP-Rap fraction (Jeon *et al.*, 2007b). Although Rap1 regulates adhesion and chemotaxis in both *Dictyostelium* and neutrophils, the spatial distribution of Rap1 activation and downstream signals is different. In *Dictyostelium*, no Radil and integrin orthologues have been identified, and Rap1-GTP is found predominantly at the leading edge, where it interacts with Phg2 and is required for myosin II assembly. In these cells Rap1-GTP is therefore poised to facilitate F-actin leading-edge protrusion by regulating myosin II assembly and disassembly (Jeon *et al.*, 2007b). In chemotaxing neutrophils, we show that the active Rap1-binding partner Radil is uniformly distributed on the plasma membrane, suggesting that active Rap1a is also uniformly distributed in these cells. Indeed, it was recently shown that the eGFP-RalGDS, a Rap1-GTP reporter (Wang *et al.*, 2006), is mostly uniformly distributed in differentiated HL-60 cells (He *et al.*, 2011). Yet we found that active β2-integrins are generally localized in the cell body and tail of polarized neutrophils. Moreover, the overexpression of either constitutively active Rap1 or Radil in neutrophils leads to the formation of very long tails during chemotaxis without obvious effects on cell protrusion or F-actin assembly. In addition, blocking integrin activation with inhibitory antibodies or inhibition of integrin signaling with FAK inhibitors is sufficient to abrogate the abnormal long-back and tail phenotype. We therefore propose that during neutrophil chemotaxis, when chemoattractant receptors and Gβγ subunits remain uniformly distributed along the plasma membrane (Chen *et al.*, 2008), Radil is recruited to the plasma membrane and, through a yet-to-be-determined mechanism, leads to the selective activation of β2-integrin at the back and sides of cells. Given that Rap1GAP is restricted to the leading edge of chemotaxing neutrophils, we envision that it specifically inhibits β2-integrin activation at the front of cells by deactivating Rap1a and Radil. Under these conditions, as Gβγ subunits remain dissociated from Gα, Radil stays associated with the plasma membrane. This spatiotemporal cycle then allows for the dynamic amoeboid migration of neutrophils to sites of inflammation.

MATERIALS AND METHODS

Reagents

fMLP was purchased from Sigma-Aldrich (St. Louis, MO), and FAK Inhibitor 14 and PF 573228 were purchased from Tocris Bioscience (Ellisville, MO). Antibodies were purchased from the following vendors: α-GFP antibody (www.jbc.org/cgi/redirect-inline?ad=Covance; Covance, Berkeley, CA), α-paxillin (pY118) and FAK (pY397) antibodies (Invitrogen, Carlsbad, CA), α-human active β1-integrin antibody for fluorescence-activated cell sorting (FACS) analyses and α-integrin β1 antibody for inhibition of β1-integrin function (Millipore, Billerica, MA), APC α-human active CD11b integrin antibody for FACS analyses of active β2-integrin (Biolegend, San Diego, CA), monoclonal α human activated CD11/CD18 clone 24 antibody for immunofluorescence of active β2-integrin (Hycult Biotech Uden, Netherlands), α-CD18 mouse monoclonal antibody for immunofluorescence of total β2-integrin

FIGURE 4: Radil and Rap1aQ63E cells exhibit enhanced β1- and β2-integrin activation. (A) Radil and Rap1aQ63E cells have enhanced β1-integrin activation. Representative flow cytometry analyses show β1-integrin activation after the addition of 1 μM fMLP. (B) Radil and Rap1aQ63E cells have enhanced β2-integrin activation. Representative flow cytometry analyses show β2-integrin activation after the addition of 1 μM fMLP. (C) Radil and Rap1aQ63E cells show enhanced paxillin phosphorylation. Cells were plated on fibronectin-coated plates for 10 min and uniformly stimulated with 1 μM fMLP, and P-paxillin levels were assessed. Quantification of three experiments is presented as the amount of P-paxillin after fMLP stimulation relative to that of unstimulated Rap1aWT cells (mean ± SD). The amount of P-paxillin at each point was standardized by dividing its value with the value of GAPDH of the same time point. $^{\#}p < 0.05$. See Supplemental Figure S4B for representative Western blot. (D) Radil and Rap1aQ63E cells show enhanced FAK phosphorylation. Cells were plated on fibronectin-coated plates for 10 min and uniformly stimulated with 1 μM fMLP, and P-FAK levels were assessed. Quantification of three experiments is presented as the amount of P-FAK after fMLP stimulation relative to that of unstimulated Rap1aWT cells (mean ± SD). The amount of P-FAK at each point was standardized by dividing its value with the value of GAPDH of the same time point. $^{\#}p < 0.05$. See Supplemental Figure S4B for representative Western blot. (E) Inhibition of FAK increases the circularity of Radil and Rap1aQ63E cells. Cells were treated with 0.5 μM FAK inhibitors as indicated, and cell circularity was quantified from the EZ-Taxiscan recordings and plotted as a function of time. Mean ± SD from six independent experiments is presented. $^{*}p < 0.01$. (F) Inhibition of FAK decreases the back and tail length of Radil and Rap1aQ63E cells. Cells were treated with FAK inhibitors as indicated, and back and tail length was quantified from EZ-Taxiscan recordings using Image J. Mean ± SD. Each point represents measurements from randomly selected cells of one experiment ($n = 20$).

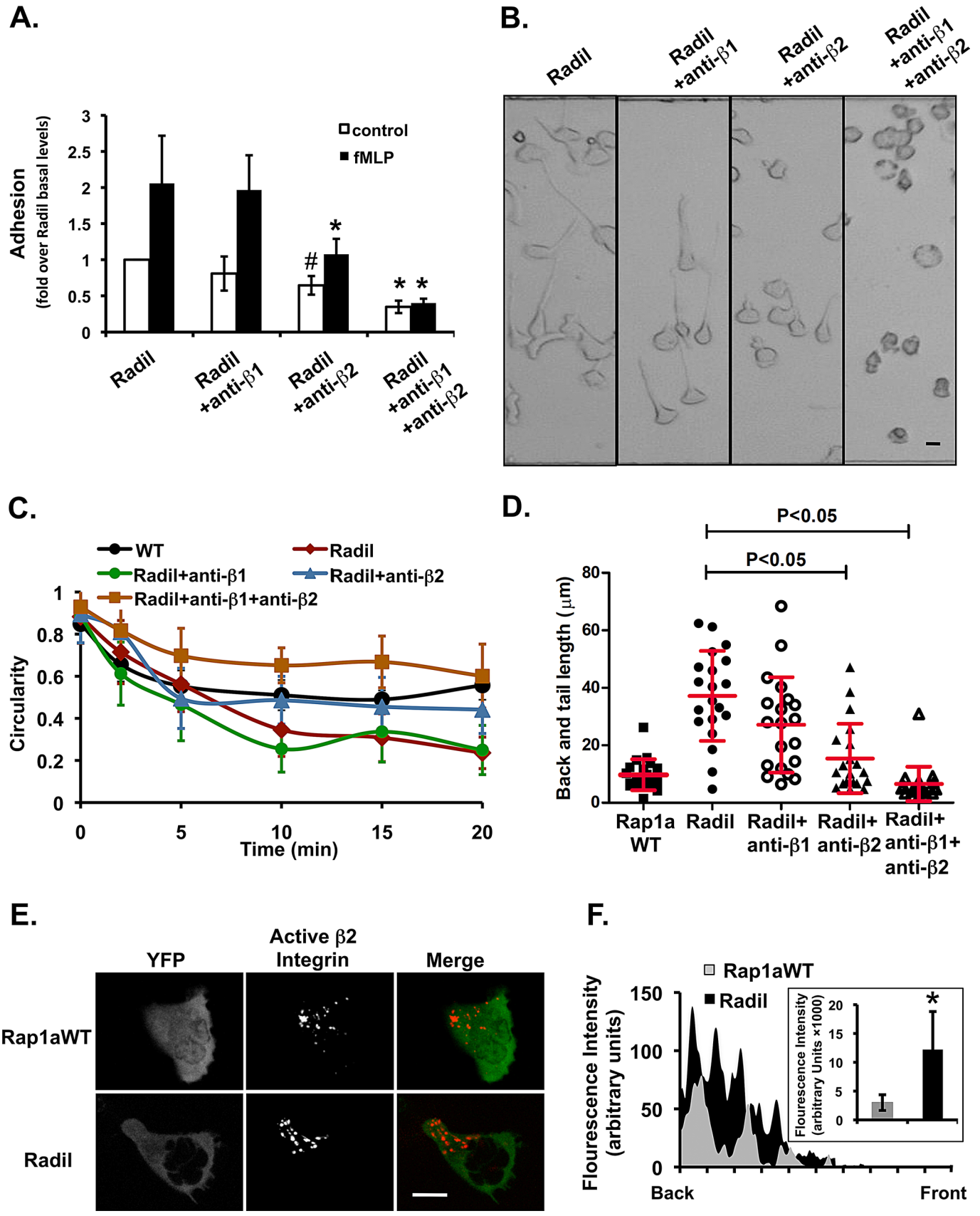

FIGURE 5: Radil regulates neutrophil adhesion and chemotaxis by activating β2-integrins. (A) The increased cell adhesion of Radil cells is inhibited by antibodies directed against β2-integrins. Cells were treated with β1-, β2-, or β1- plus β2-integrin antibodies for 1 h, and cell adhesion assays were performed as described in *Materials and Methods*. Results from three independent experiments are presented (mean ± SD). *$p < 0.01$; #$p < 0.05$. (B) The chemotaxis defect

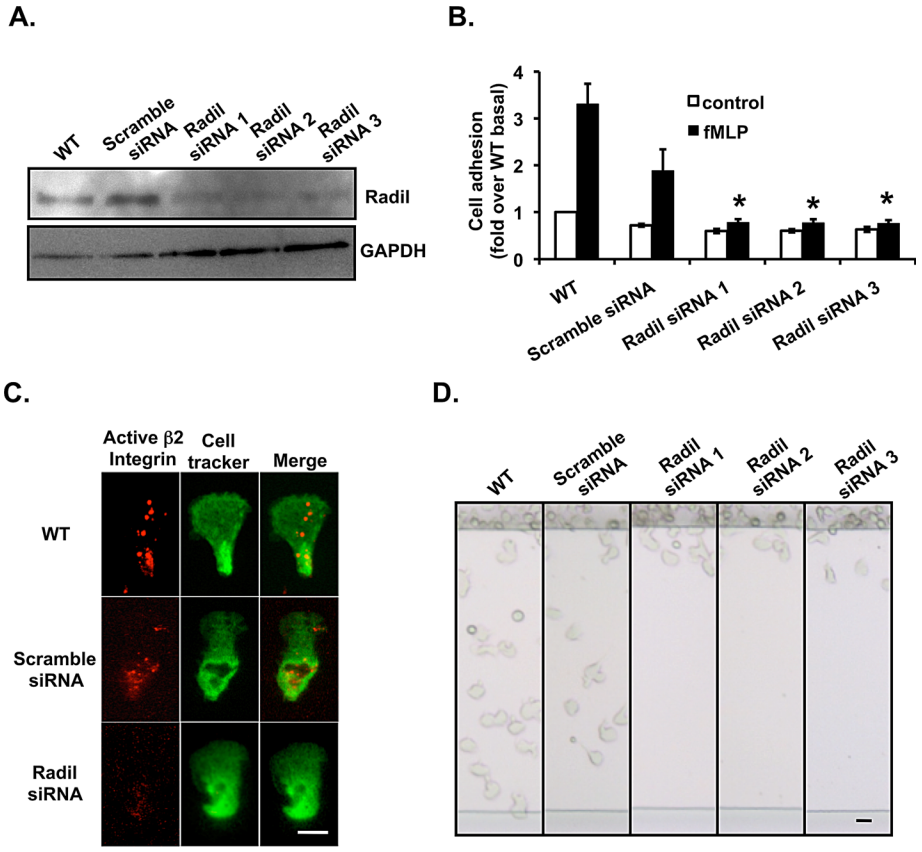

FIGURE 6: Down-regulation of Radil expression inhibits neutrophil adhesion, chemotaxis, and β2-integrin activation. (A) Scramble control siRNA and Radil-specific siRNAs were introduced into PLB-985 cells using the Amaxa Nucleofector method. The cells were harvested after 48 h, and whole-cell lysates were prepared and subjected to Western analyses using Radil-specific antibodies. A representative blot of three independent experiments. (B) Radil knockdown inhibits cell adhesion to fibronectin-coated surfaces. Cell adhesion assays were performed as described in *Materials and Methods*. Quantification of three independent experiments is presented (mean ± SD). Values are presented as fold over WT cell basal levels. $*p < 0.01$. (C) Radil knockdown reduces fMLP-induced β2-integrin activation. Cells were prestained with cell tracker green, uniformly stimulated with 1 μM fMLP for 10 min, fixed, and processed for immunofluorescence analyses. Representative fluorescence images for active β2-integrin in polarized WT, scramble siRNA, and Radil siRNA cells. Bar, 10 μm. (D) Radil knockdown inhibits neutrophil chemotaxis. Still images from EZ-Taxiscan recordings of cells. Bar, 10 μm. Also see Supplemental Movie S6.

and inhibition of β2-integrin function (www.jbc.org/cgi/redirect-inline?ad=Covance; Calbiochem, La Jolla, CA), fluorescein isothiocyanate (FITC)–rat anti–mouse IgG antibody (BD Biosciences, San Diego, CA), and phosphor-myosin light chain 2 (Ser-19) mouse monoclonal antibody (Cell Signaling Technology, Beverly, MA).

Cell lines

HEK293T cells (American Type Culture Collection, Manassas, VA) and Phoenix cells (Orbigen, San Diego, CA) were maintained on 100-mm plates in DMEM media containing 10% fetal bovine serum (FBS), 25 mM 4-(2-hydroxyethyl)-1-piperazineethanesulfonic acid (HEPES), 100 U/ml penicillin, and 100 mg/ml streptomycin at 37°C and 5% CO_2. For virus packaging, 80% confluent cells were used for transient transfection with Lipofectamine methods. PLB-985 cells were maintained in an undifferentiated state in RPMI 1640 media containing 10% FBS, 25 mM HEPES, 100 U/ml penicillin, and 100 mg/ml streptomycin at 37°C and 5% CO_2. Cells were differentiated at a density of 4.5×10^5 cells/ml for 6 d in culture media containing 1.3% dimethyl sulfoxide, and the status of differentiation was monitored by CD11b staining.

Isolation of neutrophils

Human neutrophilic polymorphonuclear leukocytes were isolated from the venous blood of healthy adults using standard dextran sedimentation and gradient separation on Histopaque 1077 (Sigma-Aldrich) as previously described (Mahadeo *et al.*, 2007; Liu *et al.*, 2010).

Plasmid constructs and transfection of PLB-985 cells

As previously described (Liu *et al.*, 2010), a retroviral approach was used to create stable populations of PLB-985 cells expressing venus, Rap1a-venus, Rap1aQ63E-venus, Rap1GAP-cerulean, and Radil-venus. The complete coding sequences of Rap1a, Rap1GAP, Rap1aQ63E, and Radil were amplified from pMT2-HA-Rap1a, pIRES-puro-Flag-Rap1GAP, pMT2-HA-Rap1aQ63E, and pIRES-puro-HA-Radil plasmids and then subcloned into pMSCVneo or pMSCVpuro retroviral vectors. The retroviral plasmids were transfected into packaging Phoenix cell lines using Lipofectamine. Transiently produced viruses were harvested after 48 or 72 h. PLB-985 cells were infected with the virus in fresh RPMI 160 culture medium containing 15 mg/ml polybrene and

of Radil cells is inhibited by treatment with β2-integrin antibodies. Still images from EZ-Taxiscan recordings of Radil cells in the presence and absence of β1- and β2-integrin antibodies. Bar 10, μm. Also see Supplemental Movie S5. (C) Inhibition of β2-integrins rescues the cell circularity defect of Radil cells. Cell circularity was quantified from the EZ-Taxiscan recordings and plotted as a function of time. Mean ± SD from three independent experiments. (D) Inhibition of β2-integrins rescues the long-tail defect of Radil cells. The length of the back and tail of the chemotaxing cells was quantified from the EZ-Taxiscan recordings using Image J. Mean ± SD. Each point represents measurements from randomly selected cells of one experiment ($n = 20$). (E) Active β2-integrins are asymmetrically distributed at the back of polarized cells. Cells were uniformly stimulated with 1 μM fMLP for 10 min, fixed, and processed for immunofluorescence analyses. Representative images for active β2-integrin in polarized Rap1aWT (top) and Radil (lower) cells. Bar, 10 μm. (F) Radil cells display higher active intracellular β2-integrin signal at the back of cells. Cells were treated as in E. The profile of fluorescence intensity of active β2-integrin signal in Rap1aWT and Radil cells was quantified using ImageJ. The average of five different cells is presented. Inset, mean ± SD active β2-integrin signal of 10 different cells.

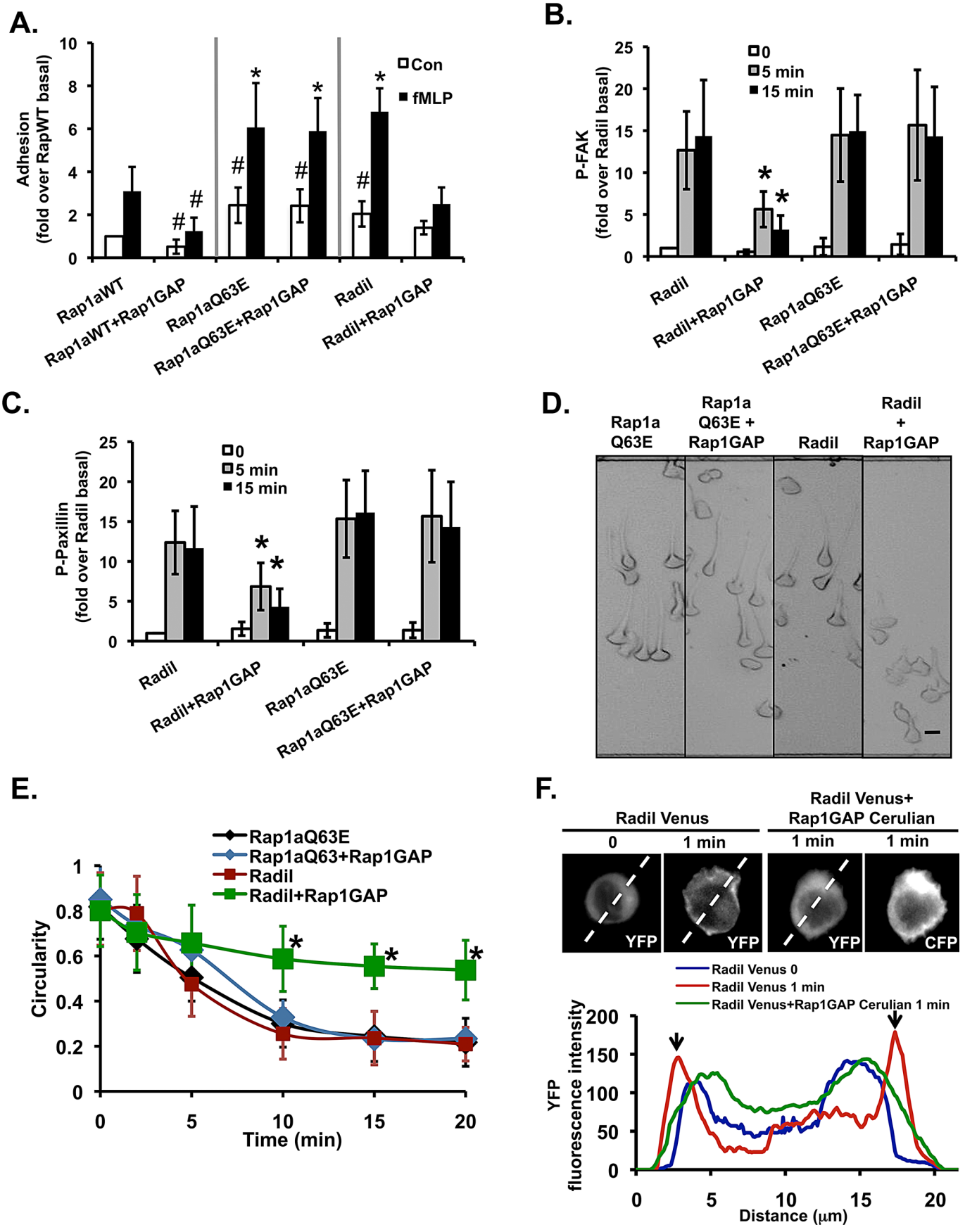
A.
Adhesion
(fold over RapWT basal)
Con
fMLP
Rap1aWT
Rap1aWT+Rap1GAP
Rap1aQ63E
Rap1aQ63E+Rap1GAP
Radil
Radil+Rap1GAP
B.
P-FAK
(fold over Radil basal)
0
5 min
15 min
C.
P-Paxillin
(fold over Radil basal)
D.
Rap1a Q63E
Rap1a Q63E + Rap1GAP
Radil
Radil + Rap1GAP
E.
Rap1aQ63E
Rap1aQ63+Rap1GAP
Radil
Radil+Rap1GAP
Circularity
Time (min)
F.
Radil Venus
Radil Venus+ Rap1GAP Cerulian
0
1 min
YFP
CFP
Radil Venus 0
Radil Venus 1 min
Radil Venus+Rap1GAP Cerulian 1 min
YFP fluorescence intensity
Distance (μm)

incubated for an additional 48 h. Cells stably expressing the genes were selected in media containing 0.6 mg/ml of G-418. Stable clonal populations were generated after 14–21 d and maintained in the selection media. Generic Radil siRNA and scrambled siRNA were purchased from Ambion (Austin, TX). PLB-985 cells were pretreated with differentiation culture medium for 3 d, and then siRNAs (4 μM) were transfected into cells using the Amaxa Nucleofector (solution V and program T-19) according to the manufacturer's protocol (Amaxa Biosystems, Lonza, Cologne, Germany). The cells were allowed to recover for an additional 2 d in differentiation culture medium and then checked for the reduction of protein expression.

Chemotaxis assay

Micropipette chemotaxis assay. Differentiated cells were plated on chambered cover slides coated with 0.2% gelatin, and a chemotactic gradient was generated using an Eppendorf microinjector with Fentotips (Eppendorf, Germany) loaded with 1 μM fMLP.

EZ-Taxiscan chemotaxis assay. The EZ-Taxiscan chamber (Effector Cell Institute, Tokyo, Japan) was assembled as described by the manufacturer. Cell migration was recorded every 15 s for 30 min at 37°C in a humidified environmental chamber. Coverslips and chips used in the chamber were coated with 1 μg/ml fibronectin or 1% bovine serum albumin at room temperature for 1 h. All glass coverslips were ultrasonicated and washed before use. Cell migration analysis was conducted using MATLAB software as previously described (Liu *et al.*, 2010).

cAMP measurement

Cells were differentiated for 5 d and starved for 24 h in reduced serum (0.2% FBS) differentiation medium and washed three times in ice-cold modified Hank's balanced salt solution (mHBSS). A total of 1×10^6 cells were lysed before and after chemoattractant stimulation. cAMP concentrations were measured using the Cell Biolabs (San Diego, CA) chemiluminescent enzyme-linked immunosorbent assay kit.

RhoA-GTP pull-down assay

The pull-down assay for RhoA-GTP was performed as described (Wojciak-Stothard *et al.*, 2007) on cells plated on fibronectin-coated 12-well tissue-culture plates after 1 μM fMLP addition. At the indicated times, cells were lysed in ice-cold lysis buffer (50 mM Tris, pH 7.2, 1% Triton X-100, 0.1% SDS, 500 mM NaCl, 10 mM $MgCl_2$, 1 mM diisopropyl fluorophosphates, protease Inhibitor cocktail, and 1 mM phenylmethylsulfonyl fluoride [PMSF]) and maintained on ice for 20 min. After centrifugation at 14,000 rpm for 10 min, the supernatants were incubated with 0.1 ml of Rhotekin RBD-agarose beads (which bind RhoA-GTP) for 1 h at 4°C, followed by three washes with Tris buffer (50 mM) containing 1% Triton X-100, 150 mM NaCl, 10 mM $MgCl_2$, 1 mM diisopropyl fluorophosphate, 0.1 mM PMSF, and protease inhibitor cocktail. Proteins bound to the beads were eluted in 2× Laemmli sample buffer and subjected to Western blot analysis by using a mouse monoclonal antibody specific for RhoA.

Isolation of cell membrane fraction

Differentiated PLB-985 venus and Radil-venus cells were uniformly stimulated with 1 μM fMLP. Aliquots of cells were taken and rapidly lysed through a 5-μm membrane at the indicated time points. The membrane fraction was isolated by centrifugation at 13,000 rpm for 20 s. The supernatant was transferred into new tube, and the pellet was resuspended in lysis buffer. The elution was subjected to SDS-PAGE and Western blot analysis with an anti-GFP or glyceraldehyde-3-phosphate dehydrogenase (GAPDH) antibody.

Morphometric analyses of cellular circularity

Cell circularity was determined using the following formula: circularity = $(4\pi \times \text{area})/\text{perimeter}^2$, which quantifies the roundness of the cell. A value approaching 1.0 is equivalent to a nearly round cell. Hence the resting neutrophils have a profile closer to 1.0 compared with long and polarized neutrophils. Digital micrographs of chemotaxing cells from EZ-Taxiscan images were taken at the indicated time points. The area and perimeter of randomly selected cells were analyzed using ImageJ (National Institutes of Health, Bethesda, MD). At least 100 cells from frames of three independent movies were analyzed. The back and tail length was measured from the EZ-Taxiscan recordings by manually selecting the center of the nucleus and the end of cells and using ImageJ to obtain a measurement of this distance. At least 20 cells from frames of representative movies were analyzed.

Cell adhesion assay

Ninety-six–well flat-bottom plates (BD Biosciences) were coated with 1 μg/ml fibronectin from human plasma (Sigma-Aldrich) for 1 h at room temperature. Wells were washed and blocked with 1% BSA

FIGURE 7: Rap1a-GTP regulates Radil activity during neutrophil adhesion and chemotaxis. (A) Rap1GAP expression restores the cell adhesion defect of Radil cells. Rap1GAP was coexpressed with Rap1aWT, Rap1aQ63E, and Radil, and cell adhesion assays were performed as described in *Materials and Methods*. Values are presented as fold over Rap1aWT cell basal levels. Quantification of three independent experiments is presented (mean ± SD). *$p < 0.01$; #$p < 0.05$. (B, C) Rap1GAP expression rescues the integrin-signaling defect of Radil cells. Cells were plated on fibronectin-coated plates for 10 min and uniformly stimulated with 1 μM fMLP. At specific time points, samples were subjected to Western blot analyses using an anti–P-FAK or P-paxillin antibodies. Quantification of three experiments is presented as the amount of P-FAK (C) or P-paxillin (D) after fMLP stimulation relative to that of unstimulated Radil cells (mean ± SD). The amount of P-FAK or P-paxillin at each point was standardized by dividing its value with the value of GAPDH of the same time point. *$p < 0.01$. See Supplemental Figure S6D for representative Western blot. (D) Rap1GAP expression rescues the chemotaxis defect of Radil cells. Still images from EZ-Taxiscan recordings of Radil and Rap1aQ63E cells with or without Rap1GAP expression. Bar, 10 μm. Also see Supplemental Movie S7. (E) Rap1GAP expression rescues the cell circularity defect of Radil cells. Cell circularity was quantified from the EZ-Taxiscan recordings and plotted as a function of time. Mean ± SD from six independent experiments. *$p < 0.01$. (F) Rap1GAP expression inhibits the fMLP-mediated translocation of Radil. Radil or Radil/Rap1GAP-coexpressing cells were uniformly stimulated with 1 μM fMLP. Still fluorescence images from time lapse. Venus fluorescence intensity was determined by line-scan analysis (white line) at the indicated time points. The arrows represent the fluorescence intensity peaks on the plasma membrane in the various frames.

in phosphate-buffered saline (PBS) for 1 h at room temperature. Then 50 µl (1×10^6 cells/ml) were seeded onto precoated plates and incubated at 37°C for 15 min. After being stimulated with fMLP at 37°C for 15 min, unattached cells were removed by gentle agitation and washed with washing buffer (0.1% BSA, 1% aprotinin in PBS) twice. Attached cells were then fixed with 4% formaldehyde and stained with crystal violet at room temperature for 10 min. The bound crystal violet was dissolved with 1% SDS and analyzed at 590 nm. Values are presented as fold over control cell basal levels. The absolute OD_{590} for Rap1aWT cells was 0.086 ± 0.006 (Supplemental Figure S3D).

Integrin activation assay

Differentiated PLB-985 cells were incubated for 1 h in the presence of α-human active β1-integrin or APC α-human active CD11b integrin antibodies. Cells were washed in mHBSS three times. Human active β1-integrin–stained cells were further incubated with FITC–rat anti-mouse IgG for 45 min, followed by three washes in mHBSS. Cells were then resuspended and analyzed by flow cytometry on a BD Biosciences FACSCalibur using BD CellQuest Pro software. Post acquisition data analysis was done using FlowJo, version 8.8.4, software.

Immunofluorescence studies

Indirect immunofluorescence analyses of F-actin and total and active β2-integrins were performed on differentiated cells or primary blood neutrophils. Briefly, cells were plated on fibronectin-coated Lab-Tek glass chamber (Nalge Nunc International, Rochester, NY) and stimulated with 1 µM fMLP in mHBSS for 10 min. Cells were fixed in 3.7% paraformaldehyde for 10 min at room temperature first and then in cold methanol at –20°C for another 10 min, followed by permeabilization with 0.2% Triton X-100 for 10 min and immunostaining with primary antibodies (1:100 dilution) or secondary antibodies for 1 h at room temperature. F-actin was assessed by incubating fixed cells with 0.2 unit of rhodamine-conjugated phalloidin at room temperature for 15 min. Fluorescence images were acquired with Zeiss Axiovert 200 (Carl Zeiss, Jena, Germany) equipped with a PE ERS6FO UltraView spinning-disk confocal system (PerkinElmer Waltham, MA) and analyzed using image J (Burgess *et al.*, 2010).

Statistical analysis

Data were tested and analyzed by one-way analysis of variance and Student's *t* test. Statistical evaluations were performed using GraphPad Software (La Jolla, CA) Prism and STATS programs. Differences with $p < 0.05$ were considered statistically significant.

ACKNOWLEDGMENTS

We thank Amy Melpolder and the National Institutes of Health Blood Bank for providing human blood from healthy volunteers. We also thank members of the Parent laboratory for excellent discussions and suggestions and, in particular Philippe Afonso and Christina Stuelten for valuable input on the manuscript. This research was supported by the Intramural Research Program of the Center for Cancer Research, National Cancer Institute, National Institutes of Health, and by a research grant to S.A. from the Canadian Breast Cancer Foundation–Ontario Chapter.

REFERENCES

Abraham RT (2002). Antigen receptors rap to integrin receptors. Nat Immunol 3, 212–213.

Abram CL, Lowell CA (2009). The ins and outs of leukocyte integrin signaling. Annu Rev Immunol 27, 339–362.

Ahmed SM, Daulat AM, Meunier A, Angers S (2010). G protein betagamma subunits regulate cell adhesion through Rap1a and its effector Radil. J Biol Chem 285, 6538–6551.

Arai A, Nosaka Y, Kanda E, Yamamoto K, Miyasaka N, Miura O (2001). Rap1 is activated by erythropoietin or interleukin-3 and is involved in regulation of beta1 integrin-mediated hematopoietic cell adhesion. J Biol Chem 276, 10453–10462.

Asha H, de Ruiter ND, Wang MG, Hariharan IK (1999). The Rap1 GTPase functions as a regulator of morphogenesis in vivo. EMBO J 18, 605–615.

Bagorda A, Parent CA (2008). Eukaryotic chemotaxis at a glance. J Cell Sci 121, 2621–2624.

Banno A, Ginsberg MH (2008). Integrin activation. Biochem Soc Trans 36, 229–234.

Berton G, Lowell CA (1999). Integrin signalling in neutrophils and macrophages. Cell Signal 11, 621–635.

Borregaard N (2010). Neutrophils, from marrow to microbes. Immunity 33, 657–670.

Bos JL (2005). Linking Rap to cell adhesion. Curr Opin Cell Biol 17, 123–128.

Bos JL, de Bruyn K, Enserink J, Kuiperij B, Rangarajan S, Rehmann H, Riedl J, de Rooij J, van Mansfeld F, Zwartkruis F (2003). The role of Rap1 in integrin-mediated cell adhesion. Biochem Soc Trans 31, 83–86.

Burgess A, Vigneron S, Brioudes E, Labbe JC, Lorca T, Castro A (2010). Loss of human Greatwall results in G2 arrest and multiple mitotic defects due to deregulation of the cyclin B-Cdc2/PP2A balance. Proc Natl Acad Sci USA 107, 12564–12569.

Burridge K, Turner CE, Romer LH (1992). Tyrosine phosphorylation of paxillin and pp125FAK accompanies cell adhesion to extracellular matrix: a role in cytoskeletal assembly. J Cell Biol 119, 893–903.

Carlos TM, Harlan JM (1994). Leukocyte-endothelial adhesion molecules. Blood 84, 2068–2101.

Caron E, Self AJ, Hall A (2000). The GTPase Rap1 controls functional activation of macrophage integrin alphaMbeta2 by LPS and other inflammatory mediators. Curr Biol 10, 974–978.

Chavakis E, Choi EY, Chavakis T (2009). Novel aspects in the regulation of the leukocyte adhesion cascade. Thromb Haemost 102, 191–197.

Chen S, Lin F, Shin ME, Wang F, Shen L, Hamm HE (2008). RACK1 regulates directional cell migration by acting on G betagamma at the interface with its effectors PLC beta and PI3K gamma. Mol Biol Cell 19, 3909–3922.

Friedl P, Wolf K (2010). Plasticity of cell migration: a multiscale tuning model. J Cell Biol 188, 11–19.

Friedl P, Zanker KS, Brocker EB (1998). Cell migration strategies in 3-D extracellular matrix: differences in morphology, cell matrix interactions, and integrin function. Microsc Res Tech 43, 369–378.

Gambardella L *et al.* (2011). The GTPase-activating protein ARAP3 regulates chemotaxis and adhesion-dependent processes in neutrophils. Blood 118, 1087–1098.

Gloerich M, Bos JL (2011). Regulating Rap small G-proteins in time and space. Trends Cell Biol 21, 615–623.

Guan JL (1997). Role of focal adhesion kinase in integrin signaling. Int J Biochem Cell Biol 29, 1085–1096.

Guo W, Giancotti FG (2004). Integrin signalling during tumour progression. Nat Rev Mol Cell Biol 5, 816–826.

Han J *et al.* (2006). Reconstructing and deconstructing agonist-induced activation of integrin alphaIIbbeta3. Curr Biol 16, 1796–1806.

He Y, Kapoor A, Cook S, Liu S, Xiang Y, Rao CV, Kenis PJ, Wang F (2011). The non-receptor tyrosine kinase Lyn controls neutrophil adhesion by recruiting the CrkL-C3G complex and activating Rap1 at the leading edge. J Cell Sci 124, 2153–2164.

Huttenlocher A, Horwitz AR (2011). Integrins in cell migration. Cold Spring Harb Perspect Biol 3, a005074.

Hynes RO (2002). Integrins: bidirectional, allosteric signaling machines. Cell 110, 673–687.

Jeon TJ, Lee DJ, Lee S, Weeks G, Firtel RA (2007a). Regulation of Rap1 activity by RapGAP1 controls cell adhesion at the front of chemotaxing cells. J Cell Biol 179, 833–843.

Jeon TJ, Lee DJ, Merlot S, Weeks G, Firtel RA (2007b). Rap1 controls cell adhesion and cell motility through the regulation of myosin II. J Cell Biol 176, 1021–1033.

Katagiri K, Hattori M, Minato N, Irie S, Takatsu K, Kinashi T (2000). Rap1 is a potent activation signal for leukocyte function-associated antigen 1 distinct from protein kinase C and phosphatidylinositol-3-OH kinase. Mol Cell Biol 20, 1956–1969.

Katagiri K, Hattori M, Minato N, Kinashi T (2002). Rap1 functions as a key regulator of T-cell and antigen-presenting cell interactions and modulates T-cell responses. Mol Cell Biol 22, 1001–1015.

Katagiri K, Maeda A, Shimonaka M, Kinashi T (2003). RAPL, a Rap1-binding molecule that mediates Rap1-induced adhesion through spatial regulation of LFA-1. Nat Immunol 4, 741–748.
Kinbara K, Goldfinger LE, Hansen M, Chou FL, Ginsberg MH (2003). Ras GTPases: integrins' friends or foes? Nat Rev Mol Cell Biol 4, 767–776.
Lafuente EM, Iwamoto Y, Carman CV, van Puijenbroek AA, Constantine E, Li L, Boussiotis VA (2007). Active Rap1, a small GTPase that induces malignant transformation of hematopoietic progenitors, localizes in the nucleus and regulates protein expression. Leuk Lymphoma 48, 987–1002.
Lafuente EM, van Puijenbroek AA, Krause M, Carman CV, Freeman GJ, Berezovskaya A, Constantine E, Springer TA, Gertler FB, Boussiotis VA (2004). RIAM, an Ena/VASP and profilin ligand, interacts with Rap1-GTP and mediates Rap1-induced adhesion. Dev Cell 7, 585–595.
Liu L, Das S, Losert W, Parent CA (2010). mTORC2 regulates neutrophil chemotaxis in a cAMP- and RhoA-dependent fashion. Dev Cell 19, 845–857.
Liu L, Parent CA (2011). Review series: TOR kinase complexes and cell migration. J Cell Biol 194, 815–824.
Lundberg S, Lindholm J, Lindbom L, Hellstrom PM, Werr J (2006). Integrin alpha2beta1 regulates neutrophil recruitment and inflammatory activity in experimental colitis in mice. Inflamm Bowel Dis 12, 172–177.
Mahadeo DC, Janka-Junttila M, Smoot RL, Roselova P, Parent CA (2007). A chemoattractant-mediated Gi-coupled pathway activates adenylyl cyclase in human neutrophils. Mol Biol Cell 18, 512–522.
Mambole A, Bigot S, Baruch D, Lesavre P, Halbwachs-Mecarelli L (2010). Human neutrophil integrin alpha9beta1: up-regulation by cell activation and synergy with beta2 integrins during adhesion to endothelium under flow. J Leukoc Biol 88, 321–327.
Mitra SK, Schlaepfer DD (2006). Integrin-regulated FAK-Src signaling in normal and cancer cells. Curr Opin Cell Biol 18, 516–523.
Niggli V (1999). Rho-kinase in human neutrophils: a role in signalling for myosin light chain phosphorylation and cell migration. FEBS Lett 445, 69–72.
Nitta N, Tsuchiya T, Yamauchi A, Tamatani T, Kanegasaki S (2007). Quantitative analysis of eosinophil chemotaxis tracked using a novel optical device—TAXIScan. J Immunol Methods 320, 155–163.
Parkinson K, Bolourani P, Traynor D, Aldren NL, Kay RR, Weeks G, Thompson CR (2009). Regulation of Rap1 activity is required for differential adhesion, cell-type patterning and morphogenesis in *Dictyostelium*. J Cell Sci 122, 335–344.
Pierini LM, Lawson MA, Eddy RJ, Hendey B, Maxfield FR (2000). Oriented endocytic recycling of alpha5beta1 in motile neutrophils. Blood 95, 2471–2480.
Raaijmakers JH, Bos JL (2009). Specificity in Ras and Rap signaling. J Biol Chem 284, 10995–10999.
Rebstein PJ, Cardelli J, Weeks G, Spiegelman GB (1997). Mutational analysis of the role of Rap1 in regulating cytoskeletal function in *Dictyostelium*. Exp Cell Res 231, 276–283.
Rebstein PJ, Weeks G, Spiegelman GB (1993). Altered morphology of vegetative amoebae induced by increased expression of the *Dictyostelium discoideum* ras-related gene rap1. Dev Genet 14, 347–355.
Reedquist KA, Ross E, Koop EA, Wolthuis RM, Zwartkruis FJ, van Kooyk Y, Salmon M, Buckley CD, Bos JL (2000). The small GTPase, Rap1, mediates CD31-induced integrin adhesion. J Cell Biol 148, 1151–1158.
Rose DM, Alon R, Ginsberg MH (2007). Integrin modulation and signaling in leukocyte adhesion and migration. Immunol Rev 218, 126–134.
Sebzda E, Bracke M, Tugal T, Hogg N, Cantrell DA (2002). Rap1A positively regulates T cells via integrin activation rather than inhibiting lymphocyte signaling. Nat Immunol 3, 251–258.
Shimonaka M, Katagiri K, Nakayama T, Fujita N, Tsuruo T, Yoshie O, Kinashi T (2003). Rap1 translates chemokine signals to integrin activation, cell polarization, and motility across vascular endothelium under flow. J Cell Biol 161, 417–427.
Smolen GA, Schott BJ, Stewart RA, Diederichs S, Muir B, Provencher HL, Look AT, Sgroi DC, Peterson RT, Haber DA (2007). A Rap GTPase interactor, RADIL, mediates migration of neural crest precursors. Genes Dev 21, 2131–2136.
Suga K, Katagiri K, Kinashi T, Harazaki M, Iizuka T, Hattori M, Minato N (2001). CD98 induces LFA-1-mediated cell adhesion in lymphoid cells via activation of Rap1. FEBS Lett 489, 249–253.
Thomas JW, Cooley MA, Broome JM, Salgia R, Griffin JD, Lombardo CR, Schaller MD (1999). The role of focal adhesion kinase binding in the regulation of tyrosine phosphorylation of paxillin. J Biol Chem 274, 36684–36692.
Tohyama Y, Katagiri K, Pardi R, Lu C, Springer TA, Kinashi T (2003). The critical cytoplasmic regions of the alphaL/beta2 integrin in Rap1-induced adhesion and migration. Mol Biol Cell 14, 2570–2582.
Tucker KA, Lilly MB, Heck L, Jr, Rado TA (1987). Characterization of a new human diploid myeloid leukemia cell line (PLB-985) with granulocytic and monocytic differentiating capacity. Blood 70, 372–378.
Wang F (2009). The signaling mechanisms underlying cell polarity and chemotaxis. Cold Spring Harb Perspect Biol 1, a002980.
Wang Z, Dillon TJ, Pokala V, Mishra S, Labudda K, Hunter B, Stork PJ (2006). Rap1-mediated activation of extracellular signal-regulated kinases by cyclic AMP is dependent on the mode of Rap1 activation. Mol Cell Biol 26, 2130–2145.
Webb DJ, Donais K, Whitmore LA, Thomas SM, Turner CE, Parsons JT, Horwitz AF (2004). FAK-Src signalling through paxillin, ERK and MLCK regulates adhesion disassembly. Nat Cell Biol 6, 154–161.
Wojciak-Stothard B, Torondel B, Tsang LY, Fleming I, Fisslthaler B, Leiper JM, Vallance P (2007). The ADMA/DDAH pathway is a critical regulator of endothelial cell motility. J Cell Sci 120, 929–942.
Wright HL, Moots RJ, Bucknall RC, Edwards SW (2010). Neutrophil function in inflammation and inflammatory diseases. Rheumatology (Oxford) 49, 1618–1631.
Xu J, Wang F, Van Keymeulen A, Herzmark P, Straight A, Kelly K, Takuwa Y, Sugimoto N, Mitchison T, Bourne HR (2003). Divergent signals and cytoskeletal assemblies regulate self-organizing polarity in neutrophils. Cell 114, 201–214.